Dielectric Studies of Heterogeneous Phase Polymer Systems. Poly(ethylene oxide) Inclusions in Polycarbonate: A Model System

David Hayward, Richard A. Pethrick,* and Tiwaporn Siriwittayakorn†

Department of Pure and Applied Chemistry, University of Strathclyde, Thomas Graham Building, Cathedral Street, Glasgow G1 1X1, Scotland

Received July 10, 1991; Revised Manuscript Received November 1, 1991

ABSTRACT: Dielectric measurements are reported on a series of model sandwich structures which mimic heterophase polymer systems which have been studied in an attempt to explore the possible use of this technique for morphological characterization. The model system consists of a polycarbonate sheet into which have been introduced a large number of small diameter holes, which are in turn filled with air, poly(ethylene oxide), and triflate-doped poly(ethylene oxide). A comparison is made between the dielectric behavior of this model system and that of a similar structure in which the same volume fraction of the conducting phase is incorporated in terms of a single hole. Measurements are also reported on pure poly(ethylene oxide) in the form of pressed and molded disks. In all cases, good agreement was found between the predictions of the simple Maxwell–Wagner–Sillars theory and experimental observation. This study illustrates the potential of dielectric measurements in the investigation of conducting occlusions in a nonconducting matrix and opens up the possibility of the investigation of heterophase systems.

Introduction

Dielectric studies of phase-separated dipolar polymer systems are complicated by the presence of additional dispersions associated with *interfacial polarization* phenomena.[1-15] Detailed studies of these features have been limited by the problem of separation of the effects of blocking electrode effects[13-15] from those associated with conductive inclusions. Theoretical models for both these phenomena have developed over the last 40 years,[5,10-12] however, very few attempts have been made to test these models or to explore in detail the interfacial polarization phenomena. The phenomena have been observed in polymer emulsions,[16-23] microcapsules,[24,25] rocks,[26-30] biological cell suspensions,[31,32] heterogeneous gels,[33,34] suspensions,[35,36] polystyrene particles suspended in an electrolyte,[36,37] polyethylene films–KCl aqueous solutions,[37] water-in-oil emulsions,[11] and dispersions of Pyrex in water.[38] The classic studies were those of Sillars on salt solutions dispersed in paraffin wax and copper phthalocyanine needles dispersed in a nonpolar polymer.[11] These models illustrate the existence of an interfacial polarization phenomena distinct from that associated with blocking electrode effects; however, they all have a liquid as one of the phases and are very different systems from those encountered in phase-separated polymer systems.

A study of styrene–butadiene–styrene doped with benzoic acid[12,39] indicated that it was possible to observe interfacial polarization processes directly related to the phase-separated character of the polymer solid. In many heterophase systems, interfacial polarization processes often overlap with those associated with blocking electrodes and ionic conductivity. In principle, it is possible to separate the contribution of ionic conductivity from the other processes because the former adds to the dielectric loss but does not contribute to the dielectric permittivity. Blocking electrode effects are, however, more difficult to separate, having dispersion characteristics similar to those associated with the occurrence of conducting inclusions.

In this paper, an attempt is made to create model systems which will allow the basis of the interfacial polarization phenomena to be unambiguously tested. In a previous paper,[40] the dielectric characteristics of carbon fibers dispersed in epoxy resins were reported and indicated that the associated dielectric dispersion lies in the gigahertz frequency range. The theory of the interfacial polarization effect due to Maxwell, Wagner, and Sillars (MWS) has been modified by a number of workers[5-7,11] but depends essentially on four variables: the volume fraction of the conducting phase, its geometry defined in terms of the length-to-breadth aspect ratio in the electric field direction, the dielectric permittivity of the nonconducting matrix, and the conductivity of the occluded phase. Additional terms have been added which allow for differences in the conductivity of the interfacial region and particular features of the conduction processes in the conducting phase. While these theories add rigor to the theory, they add additional arbitrary parameters which allow the theory to be fitted to any observed process. If the validity of the MWS approach can be proven, then in principle it is possible to use the dielectric data to provide information on the *morphological structure* of phase-separated systems. This paper attempts to generate a model system which allows the simple MWS theory to be tested in a realistic manner. A number of simple models were investigated, and of these the most successful was based on inclusions of ionically doped poly(ethylene oxide) in a polycarbonate matrix.

Theory of Dielectric Dispersion in Heterogeneous Polymer Systems

Theories appropriate for the modeling of heterogeneous polymer systems have been reviewed elsewhere.[4,7,39] Of the simple theories that due to Sillars[11] is appropriate for a small volume fraction of inclusions distributed in an insulating matrix. The dielectric increment has the form

$$\Delta\epsilon = \epsilon_s - \epsilon_\infty = (v/A)\epsilon_m \quad (1)$$

where ϵ_s and ϵ_∞ are respectively the low- and high-frequency limiting values of the dielectric constant, v is the volume fraction of the conducting inclusion, A is the depolarization factor along the axis of the applied electric field, and

* To whom all correspondence should be addressed.
† Present address: Department of Chemistry, Faculty of Science, Chiang Mai University, Chiang Mai 50002, Thailand.

0024-9297/92/2225-1480$03.00/0

ϵ_m is the dielectric constant of the insulating matrix. The location of the process is defined in terms of its characteristic relaxation time τ, which has the form

$$\tau = \epsilon_m \epsilon_0 / A\sigma \quad (2)$$

where σ is the conductivity of the occlusion and ϵ_0 is the permittivity of free space (8.854 pF/m). Exact solutions have been obtained for various forms of the occlusion:

(I) prolate spheroids ($a > b$), where a and b are respectively the length and breadth of the spheroid in the direction of the field axis and A has the form

$$A = \frac{-1}{(a/b)^2 - 1} + \frac{(a/b)}{[(a/b)^2 - 1]^{3/2}} \ln \{(a/b) + [(a/b)^2 - 1]^{1/2}\} \quad (3)$$

(II) oblate spheroids ($a < b$)

$$A = \frac{1}{1 - (a/b)^2} + \frac{(a/b)}{[1 - (a/b)^2]^{3/2}} \arccos (a/b) \quad (4)$$

(III) sphere ($a = b$), $A = {}^1/_3$.

The above equations need to be combined with the Debye equations to allow prediction of the frequency dependence of the dielectric response

$$\epsilon'(\omega) = \epsilon_\infty + \frac{\epsilon_0 - \epsilon_\infty}{(1 + \omega^2\tau^2)} \quad (5)$$

and

$$\epsilon''(\omega) = \frac{(\epsilon_0 - \epsilon_\infty)\omega\tau}{(1 + \omega^2\tau^2)} \quad (6)$$

where $\epsilon'(\omega)$ and $\epsilon''(\omega)$ are respectively the frequency-dependent parts of the real and imaginary components of the complex permittivity, and ω is the angular frequency. In a real system it is reasonable to expect that the occlusions will not all be of the same size and that there should be a distribution of both a/b ratios and volume fractions present, and this can be achieved by assuming that the observed process is the superposition of a series of overlapping Debye relaxations. A computer program was written to allow simulation of the theoretical curves defined by the above equations, the input parameters being the conductivity of the occluded phase, the a/b ratio, the volume fraction of the occlusions, and the dielectric constant of the surrounding media.

Selection of a Model Heterogeneous System

A number of model systems were investigated in an attempt to obtain a suitable test for the heterophase theory. In choosing the model it was considered important to be able to determine accurately the a/b ratio, the volume fraction of the conducting phase, and the conductivity of the occluded phase. For the MWS process to lie in the available frequency range, it was desirable to have a conductance on the order of 10^{-7} $(\Omega\ m)^{-1}$. This level of conductivity is not normally available in a solid polymer which has a conductance on the order of 10^{-14} $(\Omega\ m)^{-1}$ and is best achieved by using a polymer electrolyte. There has been considerable effort in the last 10 years in the development of polymer electrolytes, and the most thoroughly investigated system is based on poly(ethylene oxide) (PEO).[41-45] In this study, we have chosen to dope PEO with lithium trifluoromethanesulfonate (triflate), which is one of the most thoroughly investigated of the available polyelectrolyte systems.[41] By correct selection of the molecular weight of the PEO and adjustment of the triflate level, it is possible to obtain the desired magnitude of conductivity so as to produce a dielectric dispersion in the correct frequency range.[46]

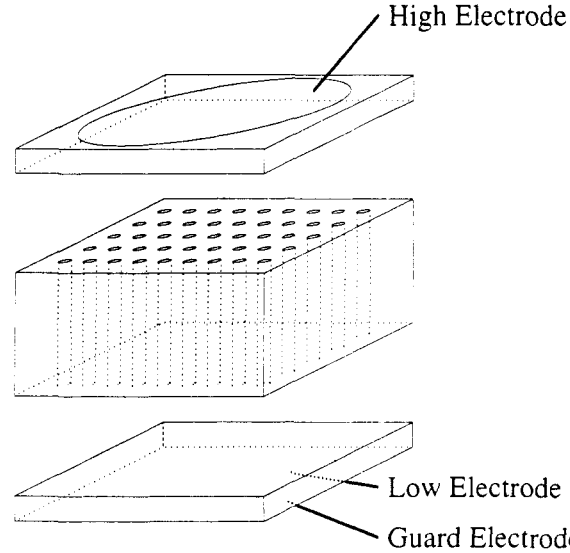

Figure 1. Schematic diagram of the polycarbonate model structure.

A number of methods were investigated for the incorporation of the conducting phase into a nonconducting polymer matrix. The first approach involved filling glass capillaries, 1 × 6 mm, with the PEO–triflate mixture, and then attempts were made to disperse these in a nonconducting matrix. The filled tubes were dispersed in a concentrated solution of polystyrene in methyl ethyl ketone, and the solvent was allowed to evaporate at room temperature. This approach was not successful because surface tension effects occurring during the evaporation process led to the tube becoming stuck together. Dispersion of the tubes in an epoxy resin was also attempted. This process proved to be tedious and difficult to achieve reproducibly, as the curing process allowed the polyelectrolyte to flow out of the capillaries.

The approach which was finally adopted involved the drilling of 210 1-mm-diameter holes in a sheet of polycarbonate (PC), 75 × 75 × 6 mm. The holes were filled with a mixture of molten PEO(8000) or molten doped (0.2% triflate) PEO(8000) and allowed to cool down to room temperature. Great care was taken to ensure that all the holes were filled. This sheet of PC was sandwiched between two other sheets of PC, 75 × 75 × 3 mm, which had been coated by evaporation using an Edwards E360A vacuum coating unit with a thin film of silver. The silver coating was then scratched out as a circular line with a diameter of 61 mm for the lower electrode and a diameter of 74 mm for the upper electrode. This structure generates a three-terminal cell configuration; the outer parts of both electrodes were connected to the earth. Shaped aluminum sheets were used to provide a Faraday screen around the electrodes and protect the silver-coated active electrodes (Figure 1). The three sheets of PC were held together using nuts and bolts at each corner, the filled holes were separated from the active electrodes by 3 mm of PC on each side, and hence there was no possibility of significant contributions from blocking electrode effects. There were 117 holes contained within the active electrode area, giving a total volume fraction of the conducting inclusions of 0.0157.

For comparison purposes a second model was generated in which, instead of using the 117 holes, a single hole of 10.8 mm diameter was drilled in the PC to be used as the center sheet. The hole was filled with PEO(8000) doped with 0.2% triflate, and this gave the same volume fraction

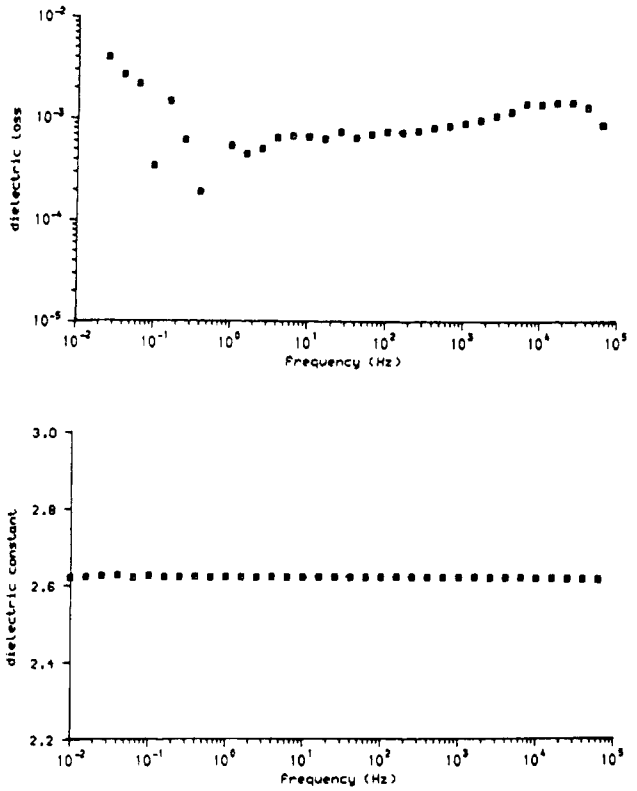

Figure 2. Dielectric constant and loss plots for the polycarbonate structure with air-filled holes.

but with a different a/b ratio.

Experimental Section

Materials. The polycarbonate used in this study was supplied in sheet form by IMI Righton, East Kilbride; lithium trifluoromethanesulfonate was obtained from Aldrich Chemical Co., and the PEO was obtained from BDH at Poole. The latter's molecular weight was determined using gel permeation chromatography, and it exhibited a melting point of 62.7 °C determined using a Du Pont DSC 9900 using a heating rate of 10 °C/min.

Conductance of the Included Phase. The conductance of each of the *holes* was measured independently using a copper electrode of a diameter identical with that of the holes through the polycarbonate sheet. The values of the conductance were determined using a Keithley 610 electrometer at room temperature.

Dielectric Measurements. Dielectric measurements were performed using a computer-assisted frequency response analysis method.[47] The dielectric permittivity $\epsilon'(\omega)$ and dielectric loss $\epsilon''(\omega)$ are calculated from the measured amplitude and phase, and the system is designed to operate over the range of 10^{-3} to 6.3×10^4 Hz. To evaluate the errors involved in the measurement, comparison is made between the dielectric response of the sample and that of an equivalent air capacitance. Phase errors can be significant below 0.1 Hz, the magnitude of the uncertainty increasing as the frequency is decreased (Figure 2).

Optical Examination of Poly(ethylene oxide). In order that the heterophase structure of the pure poly(ethylene oxide) might be determined, optical examination was carried out on pressed and molded samples of PEO(8000). The first sample was prepared in the same manner as that used for dielectric measurements and had a thickness of 0.19 mm. The second sample was obtained by melting and molding the polymer into a 0.25-mm thick sheet. Photomicrographs of both samples were taken using an Olympus CH microscope using a OM2 35-mm camera.

Poly(ethylene oxide) Pressed Disks. Because of the heterogeneous nature of poly(ethylene oxide) itself, it was appropriate to carry out an examination of the dielectric properties of the base crystalline material. A disk of PEO(8000) was prepared by pressing approximately 0.15 g of sample in a 16-mm-diameter SPECAC infrared pellet disk at a pressure of 350 bar at room temperature using an Apex type 340-4 hydraulic press. The test sample was placed between two rectangular electrodes made from copper, and the smaller lower electrode had an area of 0.95 cm^2, which was overlapped by the larger upper electrode. The sandwich was placed in the liquid-nitrogen cryostat Model DN 1704 which allowed temperature control to be achieved with a precision of ±0.1 K.

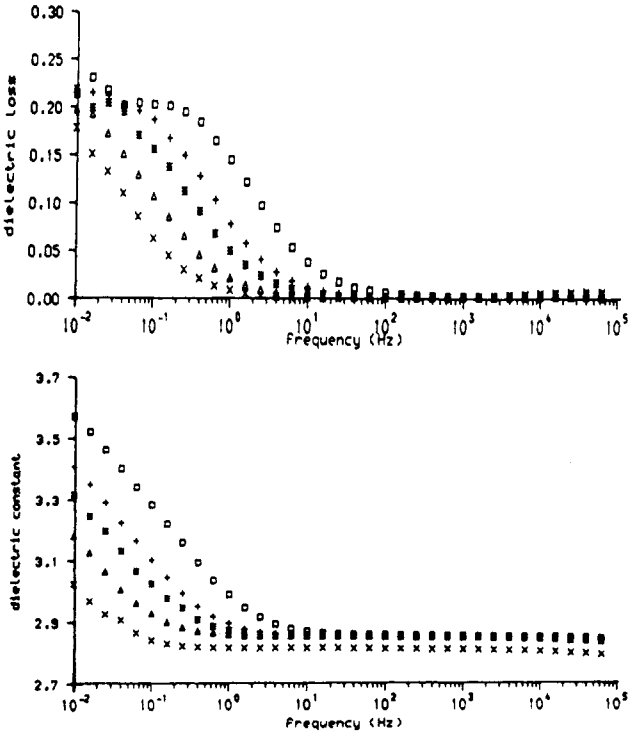

Figure 3. Dielectric constant and loss plots for the polycarbonate sheet having holes filled with PEO(8000). Key: (□) 300 K; (+) 292.3 K; (*) 228.5 K; (△) 280.2 K; (×) 278.3 K.

Results and Discussion

Dielectric Measurements on Air-Filled Inclusions. The dielectric response of the structure shown in Figure 1, with holes filled with air, was measured (Figure 2); the scatter in the data reflects the problems associated with phase errors in the network analyzer measurement at low and high frequency. As would be expected, there is no significant dielectric dispersion observed for the model system and this indicates that effects such as those associated with blocking electrodes are absent from the frequency window used in these investigations.

Dielectric Measurements on PEO-Filled Inclusions. The dielectric response of the PC sheet filled with PEO(8000) (Figure 3) indicates that the MWS dielectric process occurs toward the lower accessible frequency range of the current equipment. Substitution of the conductivity of pure PEO into eq 2 indicates that the characteristic frequency for the MWS process will lie below 10^{-3} Hz at room temperature. The observed behavior is consistent with the theory; however, it is not sufficiently accessible for accurate comparison with theory to be successfully undertaken.

Dielectric Measurements on Triflate-Doped PEO Inclusions. According to the eq 2, the dielectric relaxation can be shifted to higher frequency by increasing the conductivity of the included phase. The inclusion of triflate into PEO raises the conductivity of the inclusions to a level which will shift the MWS relaxation toward the higher frequency side of the available frequency range. Several levels of doping were investigated, and the one selected was 0.2% of triflate in PEO. The response

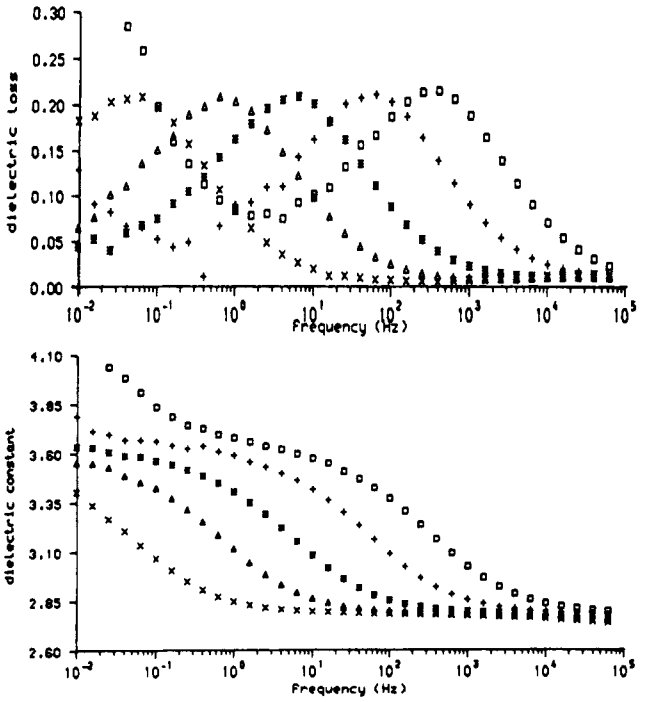

Figure 4. Dielectric constant and loss plots for the polycarbonate sheet having holes filled with 0.2% triflate-doped PEO(8000). Key: (×) 245.3 K; (△) 257.1 K; (*) 268.8 K; (+) 282.3 K; (□) 292.6 K.

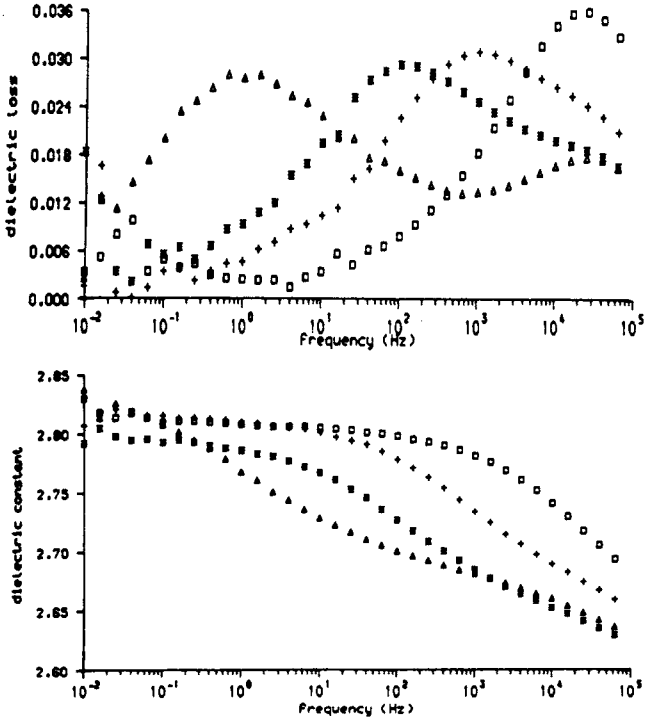

Figure 5. Dielectric constant and loss plots for the polycarbonate sheet having a 10.8-mm-diameter hole filled with 0.2% triflate-doped PEO(8000). Key: (□) 294.7 K; (+) 273.1 K; (*) 263.9 K; (△) 245.3 K.

obtained (Figure 4) was found to vary with temperature as indicated. A similar set of curves were obtained for the model system in which the central PC sheet contains only a single hole of volume equivalent to that of the separate holes in the system investigated above (Figure 5). The choice of the doping level is dictated by a compromise between the depression of the melting point achieved by increasing the triflate level and the shift of the peak which is related to the conductivity by eq 2. The physiochemical properties of triflate-doped PEO have been reported elsewhere. The variation of the conductivity of PEO and the triflate-doped PEO was measured using a compressed disk of the material used to fill the inclusions, mounted into a three-terminal configuration (Table I).

Table I
Conductivities of Molded PEO(8000) and Doped (0.2% Triflate) PEO(8000)

Molded PEO(8000)

temp, K	conductivity, $(\Omega\ m)^{-1}/10^{13}$	temp, K	conductivity, $(\Omega\ m)^{-1}/10^{13}$
321.2	65000	300.0	938
316.5	20000	292.2	186
311.6	8000	288.5	76
306.6	3000		

Doped (0.2% Triflate) PEO(8000)

temp, K	conductivity, $(\Omega\ m)^{-1}/10^{11}$	temp, K	conductivity, $(\Omega\ m)^{-1}/10^{11}$
294.7	56800	269.2	692
292.6	38200	263.9	272
282.8	7660	257.1	71
273.1	1540	245.3	6

Table II
Havriliak–Negami Curve-Fitting Parameters for the Polycarbonate Sheet Having Holes Filled with PEO(8000), Having Holes Filled with 0.2% Triflate-Doped PEO(8000), and Having a 10.8-mm-Diameter Hole Filled with Doped (0.2% Triflate) PEO(8000)

Holes Filled with PEO(8000)

temp, K	α	β	ϵ_0	ϵ_s	$\Delta\epsilon$
300	0.30	1.00	2.85	3.50	0.65
292.2	0.30	1.00	2.85	3.50	0.65
288.5	0.30	1.00	2.85	3.50	0.65

Holes Filled with 0.2% Triflate-Doped PEO(8000)

temp, K	α	β	ϵ_0	ϵ_s	$\Delta\epsilon$
292.6	0.39	1.00	2.78	3.62	0.84
282.8	0.39	0.95	2.78	3.62	0.84
268.8	0.38	0.95	2.78	3.60	0.82
257.1	0.38	0.95	2.78	3.60	0.82
245.3	0.37	0.95	2.78	3.60	0.82
calculation	0.00	1.00	2.62	3.58	0.96

10.8-mm-Diameter Hole Filled with Doped (0.2% Triflate) PEO(8000)

temp, K	α	β	ϵ_∞	ϵ_s	$\Delta\epsilon$
294.7	0.475	1.00	2.64	2.805	0.16
273.1	0.570	0.97	2.64	2.818	0.18
263.9	0.530	1.00	2.65	2.800	0.15
245.3	0.520	0.70	2.68	2.840	0.16
calculation	0.000	1.00	2.62	2.703	0.08

The observed dielectric dispersion was fitted to the Havriliak–Negami equation

$$\epsilon_r(\omega) = \epsilon_\infty + \frac{\epsilon_0 - \epsilon_\infty}{[1 + (j\omega)^{1-\alpha}]^\beta} \tag{7}$$

where α and β are parameters which are characteristic of the breadth of the distribution. The α and β parameters for the polycarbonate sheet having holes filled with PEO, the small holes filled with triflate-doped PEO, and the single large hole filled with triflate-doped PEO were obtained (Table II). The variation of the characteristic relaxation frequency (the frequency of maximum dielectric loss) with temperature for the three systems (Table III) can be represented by a simple Arrhenius type of temperature dependence[48,49]

$$\omega_c = A \exp\{-\Delta E/RT\} \tag{8}$$

where ω_c is the characteristic frequency for the relaxation

Table III
Activation Energy of Frequency at Maximum Loss ($E_{f\,max}$) of Samples Studied

sample	by	$E_{f\,max}$, kJ/mol
PC having holes filled with PEO(8000)	experiment	134
	calculation	150
PC having holes filled with doped (0.2% triflate) PEO(8000)	experiment	107
	calculation	111
PC having a 10.8-mm-diameter hole filled with doped (0.2% triflate) PEO(8000)	experiment	122
	calculation	111

at temperature T and A is the preexponential factor. The values for the systems investigated are summarized in Table III.

Discussion

At high temperatures in certain spectra are observed a second relaxation process, particularly at 292.6K in Figure 4. It is well-known that melt-crystallized PEO is highly crystalline especially for molecular weights of 4000 and above.[50-56] Several studies have been made of triflate-doped PEO, and it is found that the conducting phase is made up of three types of structure:[57] crystalline pure PEO, crystalline triflate-doped PEO, and triflate-doped amorphous PEO. Two relaxations would therefore be predicted for this system; the first, higher frequency processes are associated with the charge migration between the extremes of the hole dimensions, and a second lower frequency process is associated with the heterophase nature of the conducting phase. The form of the dielectric dispersion was calculated using eqs 1–6, using the conductivity of the sample obtained from measurements on the disk of the sample. A typical result is shown in Figure 6. The results of the calculation, based on the assumption that the inclusions approximated to prolate spheroids with a major axis "a" of 6.0 mm and a semiaxis "b" of 1.0 mm, match the observed curves in terms of the location of the dielectric dispersion. However, the shape is a very poor fit of the data. The dielectric constant of the matrix has a value of 2.62, and the volume fraction of the inclusions equals 0.0157.

Measurement of the conductivities of the individual inclusions indicated that they did *not* have the same conductivity, and the values used to fit the data are presented in Table IV. The values are grouped according to the measured conductivity into 14 sets of data, and the volume fraction reflects the number of holes with that level of conductivity. The differences in the conductivity arise as a result of the conditions used in the crystallization

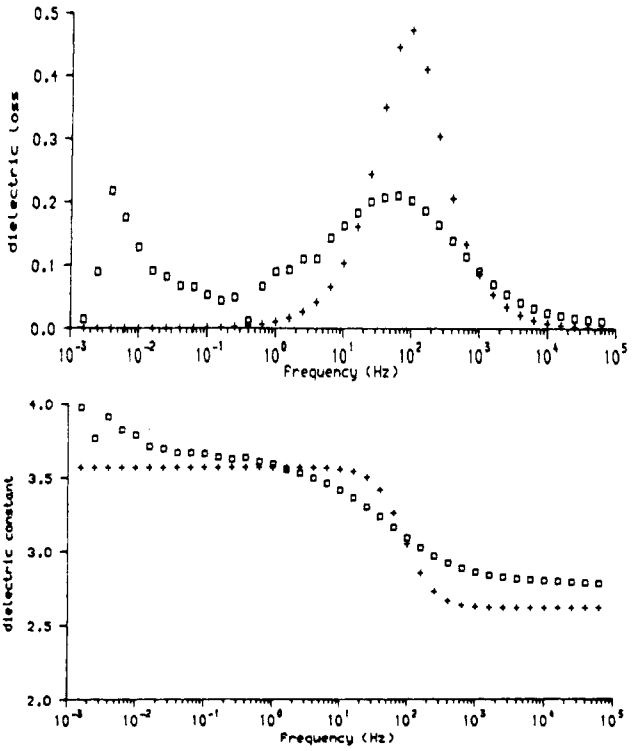

Figure 6. Comparison of the dielectric constant and loss for the polycarbonate sheet having holes filled with 0.2% triflate-doped PEO(8000) at 282.3 K. Key: (□) experiment; (+) theory.

process and reflect the differences in the percolation paths followed by the ionic conductors which produce the MWS effect. The temperature dependence of the conductivity parallels that observed in the bulk sample (Table I). The data were fitted at 292.6 K (Figure 7), and the parameters obtained were then *fixed* for subsequent calculations. The temperature dependence of τ for each of the processes was then calculated on the basis of the previously determined activation energies. The calculated curves which now contain NO ADJUSTABLE VARIABLES fit very accurately the observed curves over the temperature range 245.3–282.3 K (Figure 8). These data confirm the validity of the use of the simple MWS theory for the description of the heterophase behavior of this model system. A similar comparison of the predictions from theory and experimental data (Figure 9) for the large hole showed a similar discrepancy; however, it is not so obvious in this case how the breadth of the relaxation should be described. It is very likely that the microstructure of the doped polymer in the large hole will be different from that which exists in the smaller holes, and as a result the

Table IV
Volume Fractions and Conductivities of Doped (0.2% Triflate) PEO(8000) in the Cylinder Holes of the Polycarbonate Matrix

	proposed		estimated conductivity using Figure 3.11 at			
no.	vol. fraction	conductivity, $(\Omega\ m)^{-1}/10^{10}$ at 19.6 °C	9.8 °C $[(\Omega\ m)^{-1}/10^{10}]$	−4.2 °C $[(\Omega\ m)^{-1}/10^{12}]$	−15.9 °C $[(\Omega\ m)^{-1}/10^{12}]$	−27.7 °C $[(\Omega\ m)^{-1}/10^{14}]$
1	0.0005	5	1	10	1	8
2	0.0005	27	5	49	5	40
3	0.001	54	11	98	10	79
4	0.0005	210	43	390	41	320
5	0.00015	320	64	590	64	480
6	0.0005	380	76	690	71	560
7	0.0019	540	110	980	100	790
8	0.002	1600	320	2900	300	2400
9	0.0021	3800	760	6900	710	5600
10	0.0013	5400	1100	9800	1000	7900
11	0.001	11000	2100	19000	2100	16000
12	0.0005	16000	3200	29000	3000	24000
13	0.001	49000	9800	89000	9100	72000
14	0.0005	270000	54000	490000	50000	400000

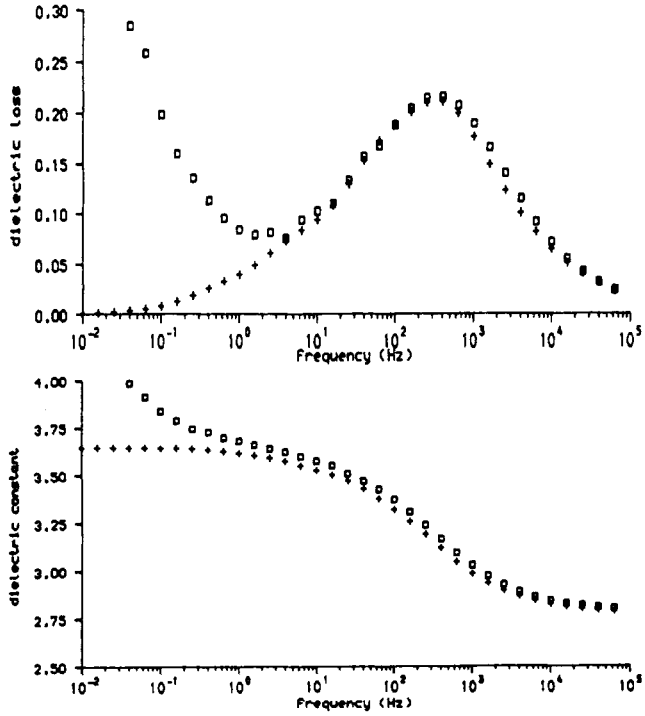

Figure 7. Comparison of dielectric loss and constant for the polycarbonate sheet having holes filled with 0.2% triflate-doped PEO(8000) at 292.6 K. Key: (□) experiment; (+) multirelaxation theory based on individual measurement of the conductivity of separate holes.

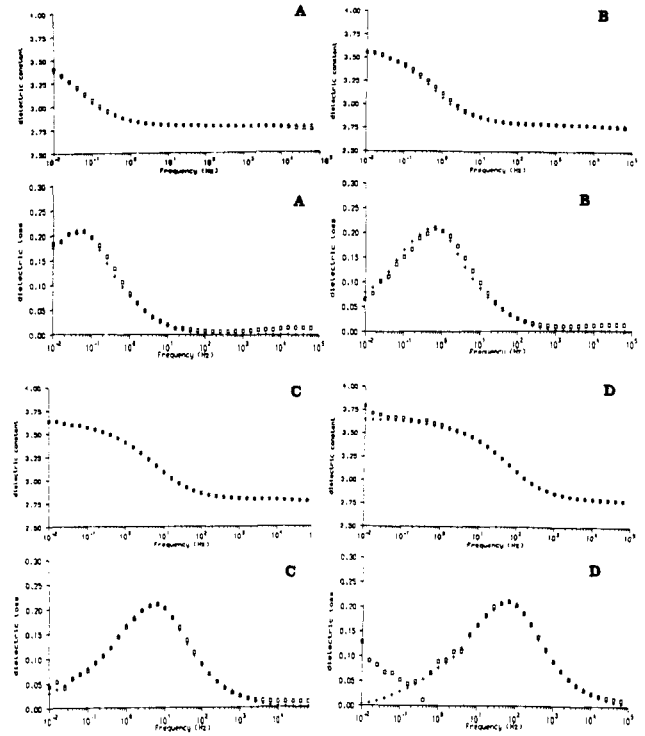

Figure 8. Comparison of the dielectric loss and constant for the polycarbonate sheet having holes filled with 0.2% triflate-doped PEO(8000) at various temperatures. Key: (A) 245.3 K; (B) 257.1 K; (C) 268.8 K; (D) 282.3 K.

percolation path followed by the ions leading to the MWS effect could be reflected in the breadth of the dispersion. It is known that in a triflate-doped PEO solid film there will exist pure PEO crystalline regions, triflate-doped crystalline regions, and amorphous regions in which will be dissolved a certain amount of triflate salt. It is therefore very probable that the occulsions are far from homogeneous and that certain of the observed deviations from the

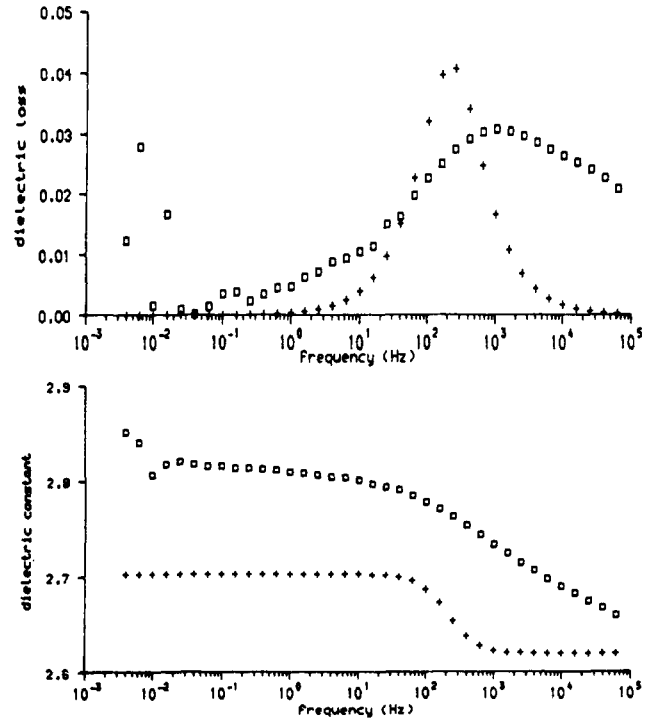

Figure 9. Comparison of dielectric constant and loss for the polycarbonate sheet having a 10.8-mm-diameter hole filled with 0.2% triflate-doped PEO (8000) at 273.1 K. Key: (□) experiment; (+) theory.

Table V
Volume Fractions and a/b of the Amorphous Regions in Crystalline PEO(8000) Pressed at 350 bar

no.	vol. fraction	a/b
1	0.0001	300
2	0.0001	250
3	0.00005	200
4	0.00033	150
5	0.0001	120
6	0.0004	100
7	0.0003	80
8	0.0024	60
9	0.005	40
10	0.003	20
11	0.005	15
12	0.001	10
13	0.002	5
14	0.003	2

expected behavior may be attributed to the heterogeneity of the doped phase.

The study of the pressed sample of PEO(8000) once more indicated the existence of a MWS process at low frequency. Optical examination of the PEO(8000) indicates that depending upon the conditions used in the crystallization the detailed nature of the crystallite structure will change and this may be expected to influence the dielectric properties of the material. Poly(ethylene oxide) forms a monoclinic crystalline phase which will be dispersed in an amorphous continuum. The conduction will occur in the amorphous phase and will be blocked by the crystalline phases. The resultant occluded structures will have a broad distribution of a/b ratios (Table V). The data (Figure 10) were modeled by a series of volume fractions and ratios, and a good fit was obtained at one temperature. As previously, the temperature dependence was then investigated using the temperature dependence of the conductivity as the only variable, and good fits were obtained. The slight deviations were within experimental error. In this latter system it is possible that electrode polarization could contribute to the observed processes. Since the forms of the loss due to the electrode polarization

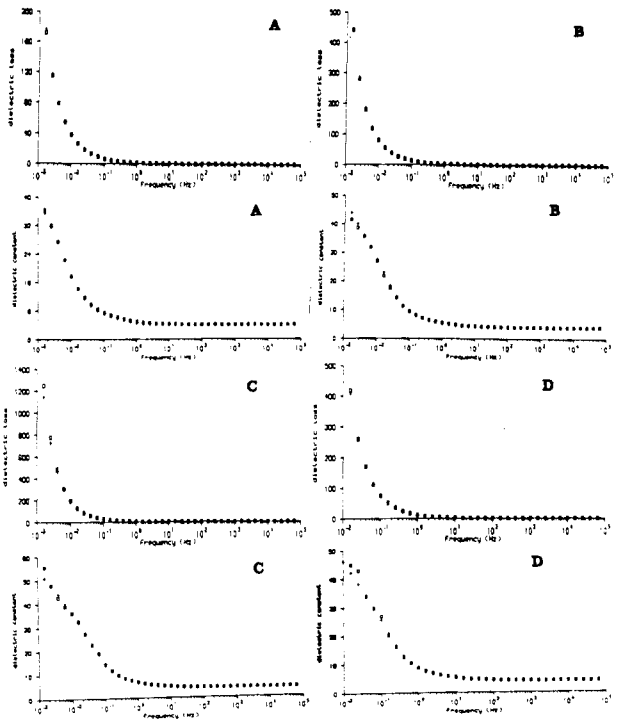

Figure 10. Comparison of dielectric constant and loss for PEO-(8000) pressed at 350 bar: experiment (□) and theory (+). Key: (A) 306.6 K; (B) 311.6 K; (C) 316.5 K; (D) 321.2 K.

and dc conduction are the same (i.e., $\alpha\omega^{-1}$), the distinction between the two processes is not very important in the estimation of the locus of the process. In this case the dielectric constant at the lowest frequencies is small relative to the dielectric loss, and this implies that the electrode polarization effects, if present, must have a relaxation time $\gg 1/(2\pi \times 10^{-3})$ s, which is lower than the frequencies for the observed MWS process. Therefore, in this case we can confidently analyze the observed process in terms of the heterogeneity of the material.

Conclusions

The experiments described above indicate that, for the model system of a conducting inclusion dispersed in a nonconducting matrix, the dielectric behavior can be accurately described by the simple MWS theory. The precision with which the curves can be predicted, in a situation where there are no adjustable parameters in the theory, demonstrates validity of the correctness of the description of the basic relaxation processes. This study indicates that it is possible to calculate the form of the morphological structure of the conducting inclusions in a nonconducting matrix from the observed dielectric dispersion data. The use of the dielectric technique to provide such information has not hitherto been appreciated as far as we are aware.

Acknowledgment. The support of the Royal Ordnance in terms of a studentship for T.S. is gratefully acknowledged.

References and Notes

(1) Daniel, V. V. *Dielectric Relaxation*; Academic Press: London, 1967.
(2) Blythe, A. R. *Electrical Properties of Polymers*; Cambridge University Press: Cambridge, U.K., 1979.
(3) Hill, N. E.; Vaughan, W. E.; Price, A. C.; Davies, M. *Dielectric Properties and Molecular Behaviour*; Van Nostrand Reinhold: London, 1969.
(4) Hedvig, P. *Dielectric Spectroscopy of Polymers*; Adam Hilger: Bristol, U.K., 1977.
(5) van Beek, L. K. H. *Prog. Dielectr.* **1967**, *7*, 69.
(6) Fricke, H. *J. Phys. Chem.* **1953**, *57*, 934.
(7) O'Konski, C. T. *J. Phys. Chem.* **1960**, *64*, 605.
(8) Maxwell, J. C. *Electricity and Magnetism*; Clarendon Press: Oxford, U.K., 1892; Vol. 1, p 452.
(9) Maxwell, J. C. *A Treatise on Electricity and Magnetism*; Clarendon Press: Oxford, U.K., 1955; Vol. 1, p 452.
(10) Wagner, K. W. *Arch. Elekrotech.* **1914**, *2*, 378.
(11) Sillars, R. W. J. *Inst. Electr. Eng.* **1937**, *80*, 378.
(12) Wilson, A. D. Ph.D. Thesis, University of Strathclyde, 1977.
(13) MacDonald, J. R. *Phys. Rev.* **1953**, *92*, 4.
(14) MacDonald, J. R.; Franceschetti, D. J. *J. Chem. Phys.* **1978**, *68*, 1614.
(15) MacDonald, J. R. *J. Electrochem. Soc.* **1988**, *135*, 2274.
(16) Hanai, T.; Imakita, T.; Koizumi, N. *Colloid Polym. Sci.* **1982**, *260*, 1029.
(17) Chen, F. P.; Chang, K. C.; Corben, L.; Falxa, M.; Levy, B. *Photogr. Sci. Eng.* **1982**, *26* (1), 15.
(18) Deinega, Yu. F.; Lobastova, A. V.; Demchenko, L. N. *Colloid J. USSR* **1983**, *45* (3), 481.
(19) Senatra, D.; Guarini, G. G. T.; Gabrielli, G.; Zoppi, M. *ACS Symp. Ser.* **1985**, *272*, 133.
(20) Senatra, D.; Gambi, C. M. C.; Neri, A. P. *J. Colloid Interface Sci.* **1981**, *79*, (2), 443.
(21) Kaneko, H.; Hirota, S. *Chem. Pharm. Bull.* **1984**, *32* (5), 1683.
(22) Kaneko, H.; Hirota, S. *Chem. Pharm. Bull.* **1983**, *31* (5), 1445.
(23) Bostock, T. A.; Boyle, M. H.; McDonald, M. P.; Wood, R. M. *J. Colloid Interface Sci.* **1980**, *73* (2), 368.
(24) Zhang, H. Z.; Sekine, K.; Hanai, T.; Koizumi, N. *Colloid Polym. Sci.* **1983**, *261*, 381.
(25) Zhang, H. Z.; Sekine, K.; Hanai, T.; Koizumi, N. *Colloid Polym. Sci.* **1984**, *262*, 520.
(26) Lysne, P. C. *Geophysics* **1983**, *48* (6), 775.
(27) Sen, P. N. *Geophysics* **1984**, *49* (5), 586.
(28) Sen, P. N. *Appl. Phys. Lett.* **1981**, *39* (8), 667.
(29) Sen, P. N. *Geophysics* **1981**, *46* (12), 1714.
(30) Sen, P. N.; Scala, C.; Cohen, M. H. *Geophysics* **1981**, *46* (5), 781.
(31) Asami, K.; Irimajiri, A.; Hanai, T.; Shiraishi, N.; Utsumi, K. *Biochim. Biophys. Acta* **1984**, *778*, 559.
(32) Asami, K.; Irimajiri, A. *Biochim. Biophys. Acta* **1984**, *778*, 570.
(33) Dissado, L. A.; Rowe, R. C.; Haidar, A.; Hill, R. M. *J. Colloid Interface Sci.* **1987**, *117* (2), 310.
(34) Rowe, R. C.; Dissado, L. A.; Zaidi, S. H.; Hill, R. M. *J. Colloid Interface Sci.* **1988**, *122* (2), 354.
(35) Ishikawa, A.; Hanai, T.; Koizumi, N. *Colloid Polym. Sci.* **1984**, *262*, 477.
(36) Hanai, T.; Sekine, K. *Colloid Polym. Sci.* **1986**, *264*, 888.
(37) Schwan, H. P.; Schwarz, G.; Maczuk, J.; Pauly, H. *J. Phys. Chem.* **1962**, *66*, 2626.
(38) Backer, R. De.; Watillon, A. *J. Colloid Interface Sci.* **1973**, *43* (2), 277.
(39) North, A. M.; Pethrick, R. A.; Wilson, A. D. *Polymer* **1978**, *19*, 913.
(40) Daly, J. H.; Hayward, D.; Pethrick, R. A. *J. Phys. D: Appl. Phys.* **1986**, *19*, 885.
(41) Vincent, C. A. *Electrochemical Science and Technology of Polymers*; Linford, R. G., Ed.; Elsevier Applied Science: London and New York, 1991; Vol. 2, p 47.
(42) Tadokoro, H. *Macromol. Rev.* **1967**, *1*, 119.
(43) Fenton, D. E.; Parker, J. M.; Wright, P. V. *Polymer* **1973**, *14*, 589.
(44) Wright, P. V. *Br. Polym. J.* **1975**, *7*, 319.
(45) Minier, M.; Berthier, C.; Gorecki, W. *J. Phys. (Paris)* **1984**, *45*, 739.
(46) McLennaghan, A. W.; Hooper, A.; Pethrick, R. A. *Eur. Polym. J.* **1989**, *12*, 1297.
(47) Hayward, D.; Mahboubian-Jones, M. G. B.; Pethrick, R. A. *J. Phys. E: Sci. Instrum.* **1984**, *17*, 683.
(48) Baird, M. E. *Electrical Properties of Polymeric Materials*; The Plastics Institute: London, 1973.
(49) Seanor, D. A. In *Polymer Science*; Jenkins, A. D., Ed.; North-Holland Publishing: Amsterdam, The Netherlands, 1972.
(50) Barnes, W. J.; Luetzel, W. G.; Price, F. P. *J. Phys. Chem.* **1961**, *65*, 1742.
(51) Hay, J. N.; Sabir, M.; Steven, R. L. T. *Polymer* **1969**, *10* (3), 187.
(52) Hay, J. N.; Sabir, M. *Polymer* **1969**, *10* (3), 203.
(53) Bailey, F. E. K., Jr.; Koleske, J. V. *Poly(Ethylene Oxide)*; Academic Press: London, 1976.
(54) Cheng, S. Z. D.; Wunderlich, B. *J. Polym. Sci., Part B: Polym. Phys.* **1986**, *24*, 577.
(55) Cheng, S. Z. D.; Wunderlich, B. *J. Polym. Sci., Part B: Polym. Phys.* **1986**, *24*, 595.
(56) Yang, M.; Salovey, R.; Allen, S. D. *J. Polym. Sci., Part B: Polym. Phys.* **1990**, *28*, 245.
(57) Cope, B. C.; Glasse, M. D. *Electrochemical Science and Technology of Polymers*; Linford, R. G., Ed.; Elsevier Applied Science: London and New York, 1991; Vol. 2, p 233.